Overall vs. local mechanical behaviour of ferritic austenitic steel joints made by laser welding

M. Iordachescu[1], A. Valiente[1] y J.L. Ocaña[2]
[1]DPTO. CIENCIA DE MATERIALES, E.T.S.I. CAMINOS, CANALES Y PUERTOS, UNIVERSIDAD POLITÉCNICA DE MADRID.
[2]CENTRO LÁSER, UNIVERSIDAD POLITÉCNICA DE MADRID.

Abstract
The present investigation addresses the overall and local mechanical performance of dissimilar joints of low carbon steel (CS) and stainless steel (SS) thin sheets achieved by laser welding in case of heat source displacement from the weld gap centreline towards CS.

Welding was performed on a Nd:YAG laser DY033 (3300 W) in a continuous wave (CW), keyhole mode. The tensile behavior of the joint different zones assessed by using a video-image based system (VIC-2D) reveals that the residual stress field, together with the positive difference in yield between the weld metal and the base materials protects the joint from being plastically deformed. The tensile loadings of flat transverse specimens generate the strain localization and failure in CS, far away from the weld.

Introduction

Joining of dissimilar metals is generally more challenging than joining similar ones because of the difference in the physical, mechanical and metallurgical properties of base materials. Thus, welding of ferritic to austenitic stainless steels is considered a major issue. In this case, the transformation strains in solid-state phase, such as austenite to martensite or ferrite during cooling and different thermal expansion coefficients result in the formation of significant residual stress. This, together with expected differences in microstructure (formation of hard zones close to the weld interface and relatively soft ones adjacent to the hard zone) may lead to crack formation at the interface and eventually to failure in service [1-5].

The present investigation addresses the overall and local mechanical performance of dissimilar joints of low carbon steel (CS) and stainless steel (SS) thin sheets achieved by laser welding in case of heat source displacement from the weld gap centreline towards CS. Welding was performed on a Nd:YAG laser DY033 (3300 W) in a continuous wave (CW), keyhole mode. The tensile behavior of the joint different zones assessed by using a video-image based system (VIC-2D) reveals that the positive difference in yield between the weld metal and the base materials protects the joint from being plastically deformed. The tensile loadings of flat transverse specimens generate the strain localization and failure in CS, far away from the weld.

Experimental set-up

The base metals (BM) employed in this study are low carbon steel (CS), AISI 1010, and austenitic stainless steel (SS), AISI 304L. Their nominal composition (in weight percent) and mechanical properties are given in **Tables 1 and 2**, respectively.

Pairs of dissimilar plates of 200 mm x 45 mm x 3 mm were butt joined by laser welding. The edges of the plates were cleaned and ground down along the weld line to ensure full contact. No special heat treatments were carried out before or after laser welding. During the welding process, the plates were firmly fixed to a specially designed clamping device [3].

Welding was performed on a Nd:YAG laser DY033 (3300 W) in a continuous wave (CW), keyhole mode. In this case, the energetic input rate of the laser welding process, η, is 50% of the laser power [4]. Helium gas was used as a

	C	Mn	Si	Cr	Cu	Ni	S	P
CS-AISI 1010	0,155	0,6	0,25	0,17	0,04	0,02	0,035	0,029
304L	0,022	1,81	0,41	18,1	0,33	9,2	0,08	0,025

Table 1. Chemical composition of the base metals [%].

	Tensile strength [MPa]	Yield strength [Mpa]	Elastic modulus [GPa]	Elongation [%]
CS-AISI 1010	365	305	190	20
304L	515	205	193	40

Table 2. Mechanical properties of the base metals.

shielding gas with a constant flow rate of 10 l/min. The laser beam position with respect to the joint groove is presented in **Figure 1**.

Standard procedures were used to prepare metallographic specimens. Macro and microstructures of the dissimilar joint were analyzed by optical microscopy after previous polishing and selective etching with aqua regia and nital 2%. Differential Interference Contrast (DIC) microscopy was used to better reveal the various mixtures of austenite and ferrite phases formed upon joint cooling.

Tensile specimens of loading direction normal to the weld, with a gauge length of 50 mm and a gauge width of 12.5 mm were machined, in accordance with ASTM E8, from the LW joint panels and native base metal plates.

Tensile testing was performed at room temperature on a 200 kN servo-hydraulic universal testing machine using a constant crosshead speed of 1 mm/min. A Video Image Correlation system (VIC-2D) was used additionally to conventional clip-on extensometers to assess the longitudinal strain distribution during the specimens' tensile loading, over an area of interest (AOI) containing the LW joint. The results were used to obtain strain averages data vs. testing time, using "virtual extensometers", on gauge lengths comparable with the lengths of different weld regions. The average strains were mapped to the corresponding global stress levels applied by the testing machine, assuming that the transversely loaded FSW specimens were in iso-stress configuration.

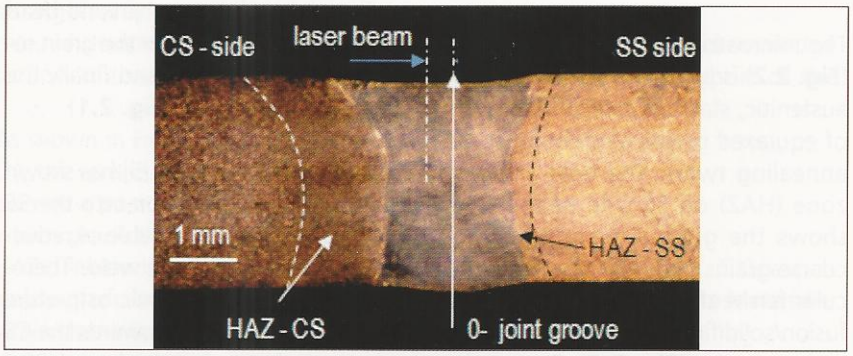

Fig. 1. Macrostructure of a dissimilar laser welded joint and the laser beam position with respect to the joint groove.

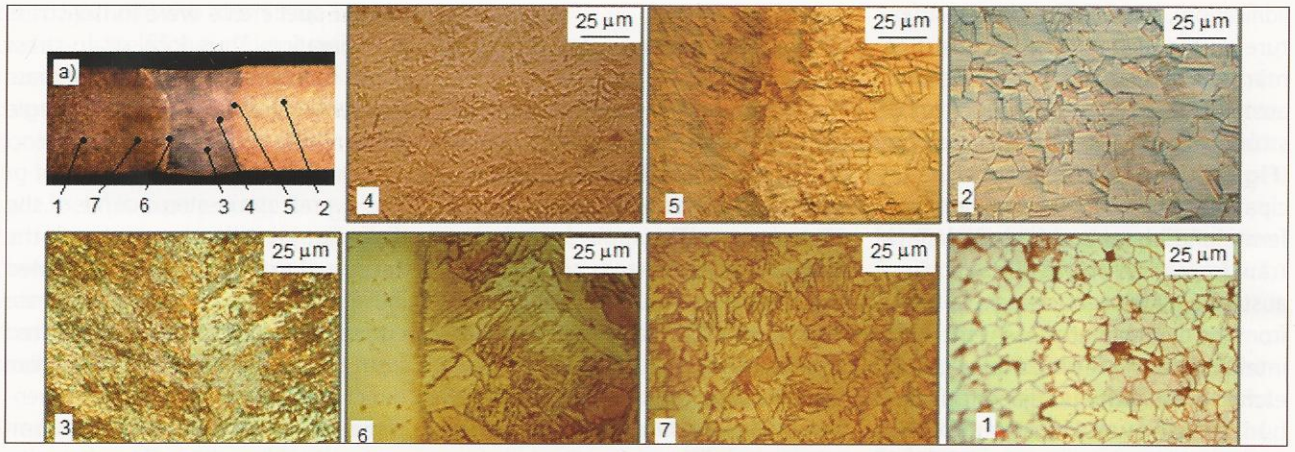

Fig. 2. Typical microstructures found into the CS-SS autogenously laser welded joints: a) microstructures position; 1- BM (CS); 2 – BM (SS); 3 – weld central region; 4 – weld microstructure close to SS; 5 – weld fusion line and HAZ on SS side; 6 – weld fusion line and coarse grains of HAZ on CS side; 7 – refined grain region from CS HAZ; BM- base metal.

Results and discussion

Optical microscopy

The joint macrostructure, typical of keyhole welding, is presented in **Fig. 2**. The higher thermal conductivity of the CS and the laser beam moving parallel, but displaced by 0.25 mm from the joint groove, explain the formation of a larger HAZ on its side. Overall, the joint microstructure is inhomogeneous, due to the different properties of base materials and laser processing characteristics, i.e. fast welding speed and low heat input. The laser beam displacement on the CS side emphasizes the differences on dilution degrees of the base metals. Details of the dissimilar joint microstructure features are presented in **Figs. 2.1-2.7**.

The microstructure of the parent SS (**Fig. 2.2**) is typical of most annealed, austenitic, stainless steel and consists of equiaxed grains containing some annealing twins. The heat affected zone (HAZ) on SS side of the joint shows the gradual transition from coarse grains of austenite and vermicular ferrite dendrites up to the weld fusion/solidification line characterized by lacy ferrite (**Fig. 2.5**). Due to the combined influence of the process high welding speed and the small thickness of the plates (which causes rapid solidification), the weld bead microstructure on the austenitic side consist of martensite, dispersed δ-ferrite and austenite (**Fig. 2.4**). The solidification structure of the weld central region (**Fig. 2.3**) indicates the higher participation of CS at joint formation; the ferrite undergoes a partial solid-state transformation and Widmanstatten austenite platelets nucleate and grow from the grain boundaries. At the weld interface on the ferritic side, a darkly etched area with an adjacent decarburized narrow band is found (**Fig. 2.6**). The HAZ of the carbon steel illustrates the transition from the coarse

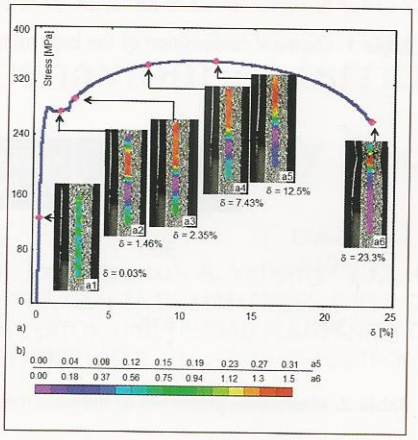

Fig.3. a) Overall stress-strain curve of the dissimilar joint; a1-a6 – VIC-2D strain maps corresponding to the specimen different elongations; b) strain legend of a5 & a6 maps.

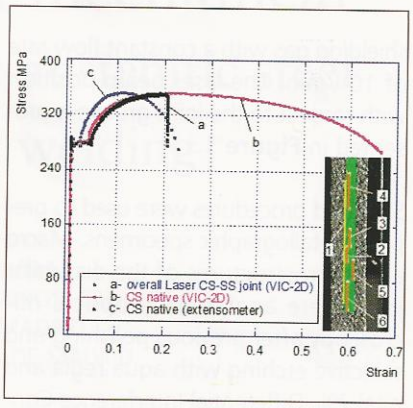

Fig.4. Engineering stress-strain curves of: a) CS using a conventional clip-on extensometer; b) CS using VIC-2D; c) CS-SS joint (overall); 1-5 - "virtual extensometers" position on joint surface.

grain microstructure region of Widmanstatten ferrite, bainite and acicular ferrite that follows the weld bead solidification front, up to the grain refined region (**Fig. 2.7**) and finally the parent CS base metal (**Fig. 2.1**).

As a recent investigation [5] has shown the martensite formation into the SS weld bead might be capable of reducing the distortion of the weld. Therefore, the resulting weld microstructure obtained by displacing towards the CS side the trajectory of the laser beam might be beneficial for producing dissimilar laser welds.

Optical microscopy

Fig. 3 presents the overall stress-strain curve of the dissimilar joint obtained during the tensile loading of the dissimilar laser welded joint using the VIC-2D technique. The strain analysis was made on digital images continuously acquired at every 0.5s. The failure of the specimen was recorded at an overall elongation of 23.3% in CS, far away from the weld (**Fig. 3-a6**). The images a1-a6 (**Fig. 3a**), shows the strain distribution at different specimens' elongation: a1- during yielding (δ=0.03%), a2 - within the yielding plateau (δ=1.46%), a3-4 - during the plastic flow (δ = 2.35% and 7.43%), a5 - at maximum load (δ=12.5%), and a6 - at failure (δ=23.3%). Maximum strains values, as presented in **Fig. 3b**, are located in CS, meanwhile the joint area is almost free of deformation.

As shown in **Fig. 4**, VIC-2D dedicated software was used to simulate 6 "virtual extensometers" capturing different zones of the joint. The strains were obtained by averaging the displacement field on the gauge length, while the stresses were conventionally computed assuming that the transversely loaded specimens were in iso-stress configuration. Thus, local strain-stress curves of different joint zones and base metals were obtained from a single tension test.

The overall strain-stress curve of the dissimilar joint (c), acquired with the 1st virtual extensometer, is presented in Fig. 4 together with the strain-stress curves of the CS base metal resulted from the VIC-2D analysis (b) and from direct measurements using a conventional clip-on extensometer (a). Comparing the (a) and (b) curves it results that VIC-2D can provide accurate in-

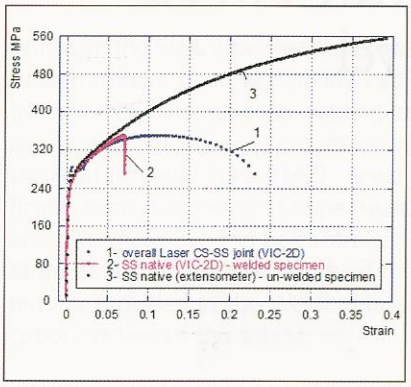

Fig.5. Engineering stress-strain curves of: 1- SS using a conventional clip-on extensometer; 2- SS using VIC-2D; 3- CS-SS joint (overall).

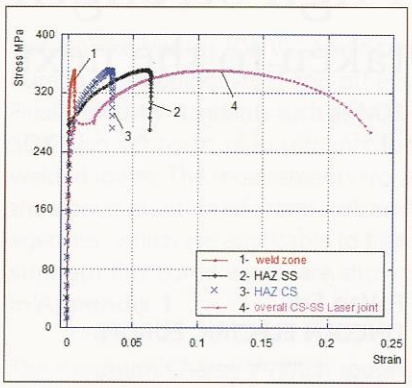

Fig.6. Engineering stress-strain curves of: 1- WZ; 2- HAZ of CS; 3- HAZ of SS; 4- CS-SS joint (overall).

formation, even after reaching the maximum load, within the plastic instabilities region, capturing the whole specimens deformation up to failure. The overall strain-stress curve (c) gives only limited information on joint specific properties, as the gauge length captures small zones of the base metals (CS and SS), the HAZs and the weld. The presence of the yielding pla-teau in the (c) curve is due to CS participation at weld formation. As the specimens´failure occurs in the CS, the overall tensile strength of the joint is in fact the tensile strength of CS base metal.

Fig. 5 shows the overall strain-stress curve of the dissimilar joint (1), acquired with the first virtual extensometer, together with the strain-stress curves of the SS base metal resulted from the VIC-2D analysis (2) and from direct measurements using a conventional clip-on extensometer (3). According to the curve (2), at joint failure, SS base metal is experiencing some plastic deformation, considerable smaller than its failure strain; VIC cannot provide information beyond the specimens' failure in the CS side of the dissimilar joint.

The complex microstructure of the joint explains the different tensile behaviour of the weld zone (WZ) and of the HAZs at specimens' failure in CS base metal (**Fig. 6**). The small thickness of the plates and the laser welding velocity dictates the WZ microstructure, consisting mostly of Widmanstatten ferrite, which is highly reducing the plastic flow of this region.

As shown in Fig. 6, strain-stress curve (1), the tensile behavior of the WZ indicates a positive difference in yield, which gradually decreases into both HAZs, relatively to the correspondent yielding of the base metals. Higher strain characterize the HAZ on SS side (0.06) when comparing with the strain value found in the HAZ from the CS side (0.045) at joint failure (0.24).

Conclusions

The dissimilar austenitic-ferritic welded joint produced by displacing the laser beam towards the CS side has a complex microstructure which on cooling induces low residual stresses. VIC method was proved efficient for assessing the mechanical behavior of local zones of an inhomogeneous material, such as the laser welded dissimilar austenitic-ferritic joint. The tensile behavior of the joint different zones assessed by using the VIC method reveals that the residual stress field, together with the positive difference in yield between the weld metal and the base materials protects the joint from being plastically deformed. The tensile loadings of flat transverse specimens generate the strain localization and failure in CS, far away from the weld.

Acknowledgment

The authors gratefully acknowledge the partial financial support of the Spanish Ministerio de Ciencia e Innovación through the projects CONSOLIDER-INGENIO 2010 CSD00C-06-14102, BIA2008-06705-C02-01 and BIA 2011-26486.

Acknowledgment

The authors gratefully acknowledge the partial financial support of the Spanish Ministerio.

References

[1] A.P. Reynolds, W. Tang, T. Gnaupel-Herold and H. Prask: Scripta Materialia, 2003, (48), 1289-1294.

[2] J.R. Berretta, W. Rossi, M.D.M. Neves, I.A. Almeida, and N.D. Vieira Junior: Optics and Lasers in Engineering, 2007, (45), 960-966.

[3] M. Iordachescu, D. Iordachescu, E. Scutelnicu, J. Ruiz-Hervias, A. Valiente and L. Caballero: Sci. Technol. Weld. Join., 2010, Vol. 15, 378-385.

[4] P. W. Fuerschbach and G. R. Eisler: Sci. Technol. Weld. Join., 2002, Vol. 7, 241–246.

[5] A. A. Shirzadi, H. K. D. H. Bhadeshia, L. Karlson and P. J. Withers: Sci. Technol. Weld. Join., 2009, 14, 559–565.

■

CESOL

SOLDADURA Y TECNOLOGÍAS DE UNIÓN

134

Año XXIV
Julio/Septiembre 2013

Revista de la Asociación Española de Soldadura y Tecnologías de Unión

ASAMBLEA GENERAL EXTRAORDINARIA DE CESOL

TECHNICAL PAPERS

Overall vs. local mechanical behaviour of ferritic austenitic steel joints made by laser welding

High strength flux cored taken to the next level

ARTÍCULOS TÉCNICOS

Fabricación y soldadura de tuberías y accesorios recubiertos con aleaciones resistentes a la corrosión

Sumario

Revista trimestral órgano oficial
de la ASOCIACIÓN ESPAÑOLA
DE SOLDADURA Y TECNOLOGÍAS
DE UNIÓN-CESOL

Director
Jorge J. Huete Chugunowa

Redacción
Asociación Española
de Soldadura y Tecnologías
de Unión
Parque Tecnológico de Leganés
Margarita Salas, 16-1ª planta
28918 Leganés (Madrid)
Tel.: 914 758 307
Fax: 915 005 377
cesol@cesol.es

Consejo de Redacción
CESOL
Fernández Villaamil, Carmen
Hernán León, Elena
Isidro Torres, Santiago
López Palomo, Ignacio
Rosell González, Juan Vicente

Publieve

Edición
Publieve Ediciones, S.L.
C/ Crevillente, 7 - Local 6.
28036 Madrid

Redacción
Silvia Bernaldo de Quirós

Diseño y maquetación
Celia Baña
celia.cesol@publieve.com
Silvia Bernaldo de Quirós
silvia.cesol@publieve.com
Patricia Piney

Responsable Comercial
Josep Mª Gascón
Tfo.: 649 419 293
publicidad@jmgascon.com

Suscripciones
secretaria@publieve.com
Tfo.: 917 812 477
Fax: 917 812 478

Distribución
National Post, S.L.

Dep. Legal: B. 3186/90 -
I.S.S.N. 1130 - 0820